Dynamic and Stability Analysis of the Power System With the Control Loop of Inverter Air Conditioners

Hongxun Hui, *Student Member, IEEE*, Yi Ding, *Member, IEEE*, Tao Chen, *Member, IEEE*, Saifur Rahman, *Life Fellow, IEEE*, and Yonghua Song, *Fellow, IEEE*

***Abstract*—The power consumption of inverter air conditioners (IACs) can be regulated flexibly by adjusting the compressor's operating frequency, which has been proven suitable for providing regulation capacities to power systems. Considering the rapid phasing out of traditional generating units, massive IACs create huge alternative regulation potential. However, the impact of IACs on the power system's stability is rarely studied. To address this issue, this article proposes the modeling and control methods of IACs to provide regulation capacities to power systems. On this basis, a novel power system model with the control loop of large-scale IACs is developed, where the communication latency during the control signal transfer process is also considered. Then, the dynamic performance and steady-state errors of the novel power system are evaluated, showing that IACs can quickly participate in and smoothly withdraw from the regulation process. Furthermore, the stabilities and sensitivities of power systems with and without IACs are compared, in order to illustrate that both the stability margin and robustness of the power system can be increased via the control loop of IACs. Finally, the effectiveness of the proposed models and methods are verified by numerical studies.**

***Index Terms*—Dynamic performance, inverter air conditioner (IAC), sensitivity analysis, stability analysis.**

Manuscript received August 14, 2019; revised December 4, 2019; accepted February 10, 2020. Date of publication February 26, 2020; date of current version November 18, 2020. This work was supported by the National Natural Science Foundation China and Joint Programming Initiative Urban Europe Call (NSFC-JPI UE) under Grant 71961137004. *(Corresponding author: Yi Ding.)*

Hongxun Hui and Yi Ding are with the College of Electrical Engineering, Zhejiang University, Hangzhou 310058, China (e-mail: huihongxun@zju.edu.cn; yiding@zju.edu.cn).

Tao Chen is with the School of Electrical Engineering, Southeast University, Nanjing 211189, China (e-mail: taoc@vt.edu).

Saifur Rahman is with the Department of Electrical and Computer Engineering, Virginia Tech, Blacksburg, VA 22203 USA (e-mail: srahman@vt.edu).

Yonghua Song is with the Department of Electrical and Computer Engineering, University of Macau, Macau 999078, China, and also with the College of Electrical Engineering, Zhejiang University, Hangzhou 310027, China (e-mail: yhsong@um.edu.mo).

Color versions of one or more of the figures in this article are available online at http://ieeexplore.ieee.org.

Digital Object Identifier 10.1109/TIE.2020.2975465

I. Introduction

A. Background

THE increasing penetration of renewable energies brings more fluctuations to power systems [1], which puts forward a higher demand for regulation capacities to maintain the system balance between power generation and consumption [2]. However, traditional generating units, such as thermal units and gas turbines, are phasing out around the world [3], which are currently the main sources of regulation reserves while may become insufficient in the near future [4].

With the rapid development of the information and communication technologies [5], demand response (DR) is becoming more feasible and accordingly paid increasing attention [6]. DR is an alternative approach of traditional generating units to provide regulation services for power systems by adjusting the power consumption of loads [7], [8]. It has been proven that DR contributes to increase the stability of power systems [9] and to decrease the system operation cost under the premise of guaranteeing end-users' comfort requirements [10], [11]. Among the various demand-side resources for DR [12], inverter air conditioners (IACs) show a number of suitable characteristics for providing regulation capacities [13].

1) The power consumption of an IAC can be regulated continuously by adjusting the compressor's operating frequency, whereas traditional loads (e.g., lights, water heaters, and regular fixed speed air conditioners) can only be controlled by switching between ON- and OFF-states. Continuously regulating instead of turning OFF an IAC has less impact on end-user comfort [14].
2) IACs are proven to have less inertia and can be regulated more rapidly than traditional generating units [15], which is significant for decreasing the system's frequency deviations.
3) The market share of IACs is increasing rapidly and has exceeded that of regular fixed speed air conditioners in many countries [15]. Statistical data show that air conditioners account for around 40% of the total electricity consumption during peak hours [16], when the regulation capacities from generating units are generally most deficient.

In summary, IACs have flexible regulation characteristics and huge regulation potential exactly at this peak power time to

substitute generating units in providing regulation capacities for power systems.

B. Literature Reviews

In the existing literature, some studies on IACs can be found. In [17], the model of an IAC and its variable-speed compressor are developed, whose accuracy and effectiveness are verified by experimental data. In [18], the IAC's operating performance is analyzed with variations of the compressor's operating frequency, system cooling load, and cooling load ratio between rooms. Besides, in [19], the operating characteristics of conventional constant speed air conditioner and IAC are compared through a specialized test platform, in which the long-term, static, starting, dynamic, and shutdown conditions are all analyzed. The results show that the IAC can make the indoor temperature reach the set value more quickly with higher energy efficiency than conventional air conditioners. However, the above-mentioned studies only focus on the IAC machine itself, while they do not consider using IACs to provide regulation services for power systems.

Some other studies indeed consider the interactions of IACs with power systems. For example, a thermal model of rooms and an electric-thermal model of air conditioners are developed in [20] to provide intra-hour balancing services for power systems, in which the direct load control algorithm and temperature-priority-list method are used to dispatch air conditioners to maintain customer desired indoor temperatures and load diversities. Moreover, the appliance commitment algorithm is proposed in [21] to schedule thermostatically controlled household loads under dynamic electricity prices. Furthermore, a co-optimization method of regulation capacities and duration time is used in [16] to mitigate the rebound of air conditioners after participating in regulation services. However, the regulation services in these studies are providing operating reserves rather than frequency regulation services, and the controlled flexible loads are conventional constant speed air conditioners rather than IACs. A conventional air conditioner's operating power has only two values, i.e., the rated power and zero. Therefore, conventional air conditioners have no capability to increase power consumption, if they are operating at the rated power. However, in the case of IACs, the operating power can be regulated flexibly by adjusting the operating frequency of the compressor. Therefore, IACs are more suitable to provide regulation services for power systems, which is exactly what this article focuses on.

In [15], IACs are equivalent to traditional generators in terms of compatible dispatch with current power system models. Moreover, in [22], IACs are modeled as thermal batteries for participating in DR, in which a finite-horizon optimization model is used to dispatch IACs with lithium-ion batteries. In [23] and [24], the neural network PID controller and the dq-axis theory, respectively, are proposed to control IACs to provide active regulation power for power systems without sacrificing customers' thermal comfort. However, the above-mentioned studies are developed and tested by simulation in the time domain. The communication latency, stability, and robustness of the power systems before and after considering IACs are not studied. By contrast, this article proposes a novel power system model in the frequency domain, where the communication latency during the control process of IACs is considered. Based on the *Padé* approximant, the steady-state error, stabilities, and sensitivities of the power system models with and without IACs are studied to illustrate the effectiveness of IACs.

In summary, existing studies mainly focus on the modeling and control methods of IACs, while the dynamic performances and stability of the power system with IACs providing regulation capacities have not been studied. This research gap is precisely what this article attempts to fill.

C. Contributions

The main work and contributions of this article are summarized as follows.

1) The thermal and electric models of IACs are developed [14]. On this basis, the control method of IACs is proposed to provide regulation capacities for the power system.
2) Based on the modeling and control methods of IACs, the novel power system model with the control loop of large-scale IACs is proposed. Considering the high sensitivity of regulation services to time (e.g., primary frequency regulation is generally within 30 s) [15], the communication latency during the regulation process is also considered in this model.
3) The steady-state error of the novel power system model with large-scale IACs is evaluated after random deviations. Compared with traditional ON–OFF loads [25], [26], IACs can withdraw from the frequency regulation process smoothly with the recovery of the system balance. This proves that the regulation of IACs has less impact on customers' comfort than traditional ON–OFF loads.
4) Moreover, the closed- and open-loop transfer functions of the novel power system with IACs are obtained to analyze changes in stabilities and sensitivities. The results illustrate that the stability margin and the robustness of a power system can both be increased by using regulation capacities from IACs.
5) By employing the *Padé* approximant and the root locus method, the impact of the communication latency is further analyzed. The results show that the 3rd-order *Padé* approximant is accurate enough for analyzing the IACs' latency.

The remainder of this article is organized as follows. Section II presents the modeling and control methods of IACs. The novel power system model with the control loop of large-scale IACs is developed in Section III. The dynamic performances, stability, and sensitivity of power systems with and without IACs are studied in Section IV. The numerical studies are presented in Section V. Finally, Section VI concludes this article.

II. Modeling and Control Methods of IACs

A. Modeling of IACs

The IAC's power consumption is closely related to the thermal characteristics of the corresponding room. Based on previous

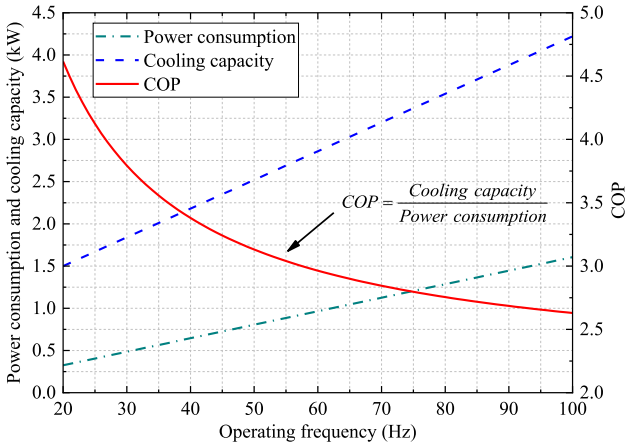

Fig. 1. Relationship of the IAC's power consumption, cooling capacity, and COP with the compressor's operating frequency.

studies [16], [20], the thermal model of the room can be expressed as

$$\frac{d\theta_i(t)}{dt} = -\frac{1}{C_i R_i}\left[\theta_i(t) - \theta_o(t) + R_i Q_i(t)\right] \tag{1}$$

where $\theta_i(t)$ is the indoor temperature in the room-*i* at time-*t*. C_i and R_i are the thermal capacity and thermal resistance of the room-*i*, respectively. $\theta_o(t)$ is the outdoor temperature at time-*t*. $Q_i(t)$ is the cooling capacity of the IAC-*i* at time-*t*.

In order to show the dynamic performances of the IAC more clearly, the time domain function (1) can be transferred to the complex frequency domain function via the *Laplace Transform*, which is described as

$$\theta_i(s) = \frac{1}{1 + C_i R_i s}\left[\theta_o(s) - R_i Q_i(s)\right] \tag{2}$$

where s is the Laplace operator.

According to the actual measurement data on the operating performance of the IAC [14], [15], the cooling capacity Q_i and the power consumption P_i will increase as the compressor's operating frequency f_i increases, as shown in Fig. 1. Q_i and P_i are regarded as being in a linear relationship with f_i. Besides, the coefficient of performance COP_i shows the relationship between the cooling capacity and the corresponding power consumption, which decreases as the compressor's operating frequency increases.

However, all these relationships in Fig. 1 are tested while the IAC operates in the steady-state. If we study the dynamic performances of the IAC, the inertia of the compressor must also be considered [15]. Because the compressor is a type of electric motor, whose operating frequency cannot be controlled and adjusted instantaneously. Therefore, by introducing the inertial element [15], [22], the cooling capacity and the power consumption of the IAC can be expressed as

$$Q_i(s) = \frac{\kappa_Q}{1 + T_c s} f_i(s) + \mu_Q \tag{3}$$

$$P_i(s) = \frac{\kappa_P}{1 + T_c s} f_i(s) + \mu_P \tag{4}$$

where T_c is the inertia time constant of the compressor. κ_Q, μ_Q, κ_P, and μ_P are the coefficients of the cooling capacity and the power consumption, respectively.

B. Control of IACs

As shown in (3) and (4), the cooling capacity and power consumption of an IAC are adjusted by regulating the compressor's operating frequency. The control objective of the operating frequency is to maintain the indoor temperature as equal to the user's set temperature. Therefore, the adjustment to the compressor's frequency is based on the gap between the indoor temperature $\Delta\theta_i(s)$ and the set temperature $\Delta\theta_{\mathrm{set},i}(s)$ [15], which can be expressed as

$$\Delta f_i(s) = C(s) \cdot \Delta\theta_{\mathrm{dev},i}(s) \tag{5}$$

$$\Delta\theta_{\mathrm{dev},i}(s) = \Delta\theta_i(s) - \Delta\theta_{\mathrm{set},i}(s) \tag{6}$$

where $C(s)$ is the inbuilt controller for regulating the compressor's operating frequency.

If the IAC can provide regulation services for power systems, the compressor's operating frequency should be controlled by the inbuilt controller $C(s)$ and an additional controller $D(s)$ for providing regulation capacities [15]. Therefore, (5) can be updated to

$$\Delta f_i(s) = C(s) \cdot \Delta\theta_{\mathrm{dev},i}(s) + D(s) \cdot \Delta f_s(s) \tag{7}$$

where $\Delta f_s(s)$ is the power system's frequency deviations.

C. Regulation Capacities Provided by IACs

The frequency regulation capacity can be evaluated based on the above models and control methods in (1)–(7). By substituting (3) into (2), the indoor temperature deviation can be obtained as

$$\Delta\theta_i(s) = \frac{1}{1 + C_i R_i s}\left[\Delta\theta_o(s) - \frac{\kappa_Q R_i}{1 + T_c s}\Delta f_i(s)\right]. \tag{8}$$

Substituting (8) into (6) and (7) yields the adjustment value of the compressor's operating frequency as follows:

$$\begin{aligned}\Delta f_i(s) = {} & \frac{(1 + T_c s)(1 + C_i R_i s) D(s)}{(1 + T_c s)(1 + C_i R_i s) + \kappa_Q R_i C(s)}\Delta f_s(s) \\ & + \frac{(1 + T_c s) C(s)}{(1 + T_c s)(1 + C_i R_i s) + \kappa_Q R_i C(s)}\Delta\theta_o(s) \\ & - \frac{(1 + T_c s)(1 + C_i R_i s) C(s)}{(1 + T_c s)(1 + C_i R_i s) + \kappa_Q R_i C(s)}\Delta\theta_{\mathrm{set},i}(s).\end{aligned} \tag{9}$$

It can be seen from (9) that the adjustment value of the compressor's operating frequency is related to three factors, the power system's frequency deviations, the outdoor temperature deviations, and the set temperature deviations. Considering the short time period of the frequency regulation process (within 30 s) [15], the outdoor temperature can be regarded as invariable during the short regulation process. Moreover, users are considered not to change the set temperature coincidently during these 30 s. Therefore, the (9) can be simplified to

$$\Delta f_i(s) = \frac{(1 + T_c s)(1 + T_a s) D(s)}{(1 + T_c s)(1 + T_a s) + \kappa_Q R_i C(s)}\Delta f_s(s) \tag{10}$$

where $T_a = C_i R_i$. Equation (10) means that the IAC compressor's operating frequency is only influenced by the power system's frequency deviation $\Delta f_s(s)$.

Substituting (10) into (4) yields the regulation capacity provided by the IAC as follows:

$$\Delta P_i(s) = \Psi(s) D(s) \Delta f_s(s) \tag{11}$$

where

$$\Psi(s) = \frac{\kappa_P (1 + T_a s)}{(1 + T_c s)(1 + T_a s) + \kappa_Q R_i C(s)}. \tag{12}$$

Compared with traditional generating units, the regulation capacity provided by one IAC is small. Therefore, the aggregated regulation capacity of the large-scale IACs is generally considered, which can be calculated by

$$\begin{aligned} \Delta P_{\mathrm{IAC}}(s) &= \sum_{i=1}^{N} \Delta P_i(s) = \sum_{i=1}^{N} \Delta P_{\mathrm{avg}}(s) S_i(s) \\ &= \Delta P_{\mathrm{avg}}(s) S_{\mathrm{ON}} \end{aligned} \tag{13}$$

where N is the total number of IACs. $\Delta P_{\mathrm{IAC}}(s)$ is the aggregated regulation capacity of IACs. As for large-scale IACs, the average regulation capacity $\Delta P_{\mathrm{avg}}(s)$ can be calculated using historical statistical data. Therefore, the total regulation capacity can also be evaluated by summing the operating state of each IAC $S_i(s)$. The $S_i(s)$ is equal to 1 if the IAC-i is in the ON-state, while it is 0 if the IAC-i is in the OFF-state. S_{ON} is the total available number of IACs in the ON-state.

III. Modeling of the Power System With the Control Loop of Large-Scale IACs

Traditional power systems are only regulated by power generation units, such as thermal units and gas turbines. Therefore, a traditional power system model without IACs can be illustrated as Fig. 2(a), where a reheat steam generator is taken as an example [27], [28].

Fig. 2(b) shows the novel power system model with the control loop of large-scale IACs [15]. The power system frequency deviation is caused by the load deviations ΔP_D and is recovered under regulation from the generator and IACs. Therefore, the system frequency deviation can be expressed as

$$\Delta f_s(s) = \frac{1}{D + 2Hs} \left[\Delta P_G(s) + \Delta \hat{P}_{\mathrm{IAC}}(s) - \Delta P_D(s) \right] \tag{14}$$

where D and H are the load-damping factor and the inertia constant of the system, respectively. $\Delta P_D(s)$ is the load deviation. $\Delta P_G(s)$ is the regulation power provided by the generator, which includes two controllers: the proportional controller $\Delta P_{GP}(s)$ for the primary frequency regulation (PFR) and the integral controller $\Delta P_{GS}(s)$ for the secondary frequency regulation (SFR). Therefore, the $\Delta P_G(s)$ can also be expressed as

$$\begin{aligned} \Delta P_G(s) &= G(s) \cdot [\Delta P_{GS}(s) - \Delta P_{GP}(s)] \\ &= G(s) \cdot \left[\Delta P_{GS}(s) - \frac{1}{R} \Delta f_s(s) \right] \end{aligned} \tag{15}$$

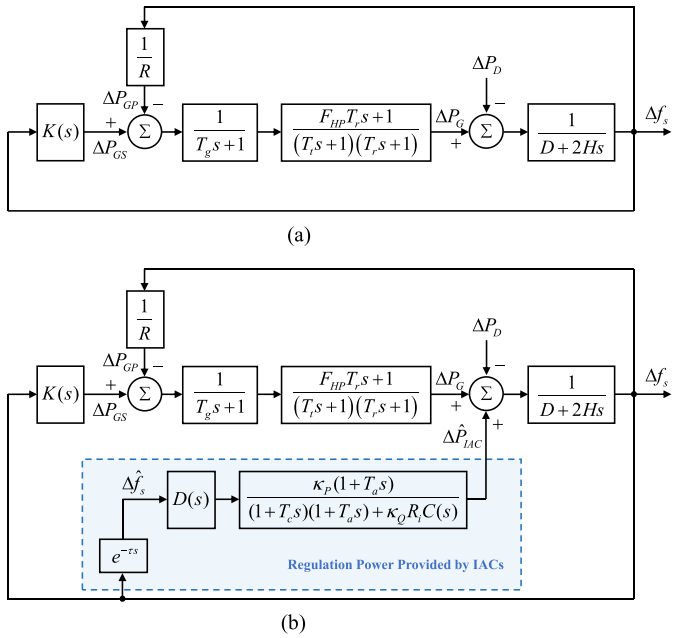

Fig. 2. Comparison of power system model with and without the control loop of IACs. (a) Traditional power system model without the control loop of IACs. (b) Novel power system model with the control loop of IACs.

where

$$G(s) = \frac{1 + F_{HP} T_r s}{(1 + T_g s)(1 + T_t s)(1 + T_r s)}. \tag{16}$$

R is the speed droop parameter. T_g, T_t, and T_r are the time constants of the speed governor, the turbine, and the reheat process, respectively. F_{HP} is the high-pressure turbine section.

As for the regulation capacities provided by the large-scale IACs, the system frequency deviations are detected first by the control center and then transmitted to each IAC's controller. This process inevitably causes the communication latency τ, which is expressed as $e^{-\tau s}$ in Fig. 2.

The communication latency process is nonlinear, which causes great inconvenience for solving the eigenvalues and analyzing the system's dynamic performances. In previous studies [25], [26], the *Padé* approximant has proven to be able to linearize the communication latency process with strong convergence results. This method is used in this article and expressed as

$$\Delta \hat{f}_s(s) = e^{-\tau s} \cdot \Delta f_s(s) \approx P_{kl}(s) \cdot \Delta f_s(s) \tag{17}$$

where

$$\begin{aligned} P_{kl}(s) &= \frac{\sum_{j=0}^{l} \frac{(l+k-j)!\, l!\, (-\tau s)^j}{j!(l-j)!}}{\sum_{j=0}^{k} \frac{(l+k-j)!\, k!\, (\tau s)^j}{j!(k-j)!}} \\ &= \frac{b_0 + b_1 \tau s + \cdots + b_l (\tau s)^l}{a_0 + a_1 \tau s + \cdots + a_k (\tau s)^k}. \end{aligned} \tag{18}$$

k and l are the orders of the denominator and numerator polynomials in the *Padé* approximant function, respectively. a_j and

b_j are the coefficients of the *Padé* approximant function, which can expressed as

$$\begin{cases} a_j = \frac{(l+k-j)!k!}{j!(k-j)!}, & j = 0, 1, \ldots, k \\ b_j = (-1)^j \frac{(l+k-j)!l!}{j!(l-j)!}, & j = 0, 1, \ldots, l \end{cases}. \tag{19}$$

Therefore, the aggregated regulation capacity of IACs can be derived from (13) and (17) into

$$\Delta \hat{P}_{\mathrm{IAC}}(s) = P_{kl}(s)\Delta P_{\mathrm{IAC}}(s). \tag{20}$$

Based on the novel power system model with the control loop of large-scale IACs, the dynamic performances, stability, and sensitivity of power systems with and without IACs are studied in Section IV.

IV. Dynamic Performance of the Power System With the Control Loop of Large-Scale IACs

A. Steady-State Error Evaluation of the Power System

As shown in Fig. 2(b), the power system frequency can be regulated by the PFR $\Delta P_{GP}(s)$ and the SFR $\Delta P_{GS}(s)$ of the generator, and the $\Delta \hat{P}_{\mathrm{IAC}}(s)$ of the IACs. Generally, the PFR is fast, while it cannot make the system frequency return to zero. Therefore, the regulation capacities will finally be provided by the SFR of the generator and the IACs in steady-state [25].

Substituting (15) and (20) into (14) yields

$$\Delta f_s(s) = \frac{1}{\Phi(s)} [G(s)\Delta P_{GS}(s) + P_{kl}(s)\Delta P_{\mathrm{IAC}}(s) - \Delta P_D(s)] \tag{21}$$

where

$$\Phi(s) = D + 2Hs + G(s)/R. \tag{22}$$

Assuming there is a step disturbance load in the power system, which can be expressed as

$$\Delta P_D(s) = \Delta P_D/s. \tag{23}$$

Then, substituting (23) into (21), the steady-state value of the system frequency deviations can be calculated as

$$\Delta f_{s,SS} = \lim_{s\to 0} s\Delta f_s(s) = \frac{1}{\Phi(0)} (\Delta P_{GS,SS} + \Delta P_{\mathrm{IAC},SS} - \Delta P_D) \tag{24}$$

where

$$\Phi(0) = D + G(0)/R = D + 1/R \tag{25}$$

$$\Delta P_{GS,SS} = \lim_{s\to 0} sG(s)\Delta P_{GS}(s) \tag{26}$$

$$\Delta P_{\mathrm{IAC},SS} = \lim_{s\to 0} sP_{kl}(s)\Delta P_{\mathrm{IAC}}(s). \tag{27}$$

Therefore, when the power system frequency returns to a steady-state, the disturbance power ΔP_D is provided by the generator $\Delta P_{GS,SS}$ and the IACs $\Delta P_{\mathrm{IAC},SS}$. The specific values of the two kinds of regulation capacities in the steady-state can be calculated as follows.

1) Steady-State Regulation Capacity of the Generator: The integral controller is generally used in the SFR process of the generator, which can be expressed as

$$\Delta P_{GS}(s) = -K\Delta f_s(s)/s. \tag{28}$$

Substituting (28) into (26) yields

$$\Delta P_{GS,SS} = -KG(0)\Delta f_s(0) = -K\int_0^\infty \Delta f_s(t)dt. \tag{29}$$

Therefore, the regulation capacity provided by the generator will increase as the system frequency deviations Δf_s increase.

2) Steady-State Regulation Capacity of the IACs: As shown in (7), there are two controllers for the IACs. The first is the inbuilt controller for maintaining the indoor temperature to be equal to the set value. The proportional-integral (PI) controller has been verified as a conventional effective method to achieve the adjustment of the compressor's operating frequency [15], which can be described as

$$C(s) = \xi + \eta/s. \tag{30}$$

The second one is the additional controller for the IAC providing regulation capacity for the power system, where the PI controller can also be adopted and can be described as

$$D(s) = -\delta - \gamma/s \tag{31}$$

where the proportional and integral gains δ and γ are set as negative values, because the IAC's operating frequency should be reduced when there is a positive disturbance load in the power system.

Substituting (30) and (31) into (11) and (12) yields the regulation capacity provided by one IAC, which is

$$\Delta P_i(s) = \frac{-\kappa_P(1+T_a s)(\delta s+\gamma)}{s(1+T_c s)(1+T_a s)+\kappa_Q R_i(\xi s+\eta)}\Delta f_s(s). \tag{32}$$

Then plugging (32) into (13) and (27), the total stable-state regulation power provided by aggregated IACs can be obtained as

$$\begin{aligned}\Delta P_{\mathrm{IAC},SS} &= \lim_{s\to 0} sP_{kl}(s) \times \sum_{i=1}^{N} \frac{-\kappa_P(1+T_a s)(\delta s+\gamma)\Delta f_s(s)}{s(1+T_c s)(1+T_a s)+\kappa_Q R_i(\xi s+\eta)} \\ &= \lim_{s\to 0} sP_{kl}(s) \sum_{i=1}^{N} \frac{-\kappa_P\gamma}{\kappa_Q R_i\eta}\Delta f_s(s) \\ &= P_{kl}(0) \sum_{i=1}^{N} \frac{-\kappa_P\gamma}{\kappa_Q R_i\eta}\Delta f_s(0) \cdot \lim_{s\to 0} s = 0.\end{aligned} \tag{33}$$

It can be seen from (33) that the IACs will finally withdraw all the regulation capacities with the recovery of the system frequency, which is exactly the ideal control result of IACs. The reason can be analyzed from (7), in which two deviations can change the operating frequency of the compressor, i.e., the temperature deviation $\Delta\theta_{\mathrm{dev},i}$ and the system frequency deviation Δf_s. When a disturbance load power occurs in the power system, the Δf_s will not be zero. Then the IAC will adjust the

compressor's operating frequency to provide regulation capacities. However, this process can also cause increases in the indoor temperature deviations $\Delta\theta_{\mathrm{dev},i}$, which will lead to the reverse regulation of the compressor's operating frequency to guarantee the indoor temperature within the acceptable ranges. Therefore, as soon as the system frequency deviation Δf_s returns to zero, the inbuilt controller $C(s)$ can make the IAC return to the original power consumption to maintain the indoor temperature. This also means that the IAC will withdraw from the regulation process at that time.

However, this does not mean that the IACs are useless for the stability of the power system. During the process of system frequency fluctuations, the IACs can rapidly adjust their power consumption to decrease the gap between the power supply side and power demand side, which is significantly helpful to reduce the system frequency deviations. The importance of the IACs to the stability and robustness of the power system will be analyzed in detail in Section IV-B.

B. Stability Analysis of the Power System With and Without IACs Providing Regulation Capacities

Based on the classical control theories [29], the stability of the power system can be characterized and analyzed by the closed-loop transfer function (CLTF) and the open-loop transfer function (OLTF). As shown in Fig. 2, the CLTF of the power system frequency deviations relating to the step disturbance load can be described as

$$\mathrm{CLTF}_{w\mathrm{IAC}}(s)=\frac{\Delta f_s(s)}{\Delta P_D(s)}=\frac{-M(s)}{\underbrace{1+M(s)\left[\left(\frac{1}{R}+\frac{K}{s}\right)G(s)+\left(\delta+\frac{\gamma}{s}\right)P_{kl}(s)\Psi(s)S_{\mathrm{ON}}\right]}_{\mathrm{OLTF}_{w\mathrm{IAC}}(s)}} \tag{34}$$

where $M(s)=(D+2Hs)^{-1}$. $\mathrm{OLTF}_{w\mathrm{IAC}}(s)$ is the open-loop transfer function for the corresponding closed-loop system.

Moreover, if there is no IAC providing regulation capacities, the CLTF of the power system can be described as

$$\mathrm{CLTF}_{wo\mathrm{IAC}}(s)=\frac{\Delta f_s(s)}{\Delta P_D(s)}=\frac{-M(s)}{\underbrace{1+M(s)\left(\frac{1}{R}+\frac{K}{s}\right)G(s)}_{\mathrm{OLTF}_{wo\mathrm{IAC}}(s)}} \tag{35}$$

where $\mathrm{OLTF}_{wo\mathrm{IAC}}(s)$ is the open-loop transfer function for the closed-loop system without IACs providing regulation services.

Based on the two open-loop transfer functions in (34) and (35), the Bode plots can be obtained to analyze the stability of the power system before and after considering IACs. Here the parameter values of the test system are based on realistic data in China [15], [16], as shown in Table I.

It can be seen from Fig. 3(a) that the gain and phase margins in the original power system without IACs are 27.4 dB and 51.6°, respectively. With the increasing number of IACs for providing regulation capacities, both the gain margin and the phase margin become larger. As shown in Fig. 3(d), when 100 000 IACs are in the control loop, the gain margin and phase margin of the power system will be 30.3 dB and 53.4°, respectively. This proves that the power system becomes more stable for dealing with uncertain load power disturbances.

TABLE I
PARAMETER VALUES OF THE TEST POWER SYSTEMS [15], [16]

Parameters	Values	Units	Parameters	Values	Units
C_i	60.55	kJ/°C	D	1.00	n/a
R_i	0.3134	°C/kW	H	10.0	n/a
θ_o	35.00	°C	T_r	7.00	s
θ_{set}	25.00	°C	T_g	0.20	s
κ_Q	0.034	kW/Hz	F_{HP}	0.30	n/a
μ_Q	0.820	kW	T_t	0.30	s
κ_P	0.016	kW/Hz	R	0.05	n/a
μ_P	0.005	kW	K	0.50	n/a
ξ	0.520	Hz/°C	T_c	0.02	s
η	0.032	Hz/(°C·s)	f_r	50	Hz
δ	200	n/a	P_r	800	MW
γ	0.02	s^{-1}	f_i	20~150	Hz

Moreover, in order to analyze the variation trends of the power system's dynamic performances with the increasing number of IACs providing regulation capacities, the root locus method is used in this article. First, the system characteristic equation (i.e., the denominator polynomial) in (34) can be rearranged as

$$\underbrace{1+S_{\mathrm{ON}}\cdot\frac{M(s)\left(\gamma+\delta s\right)P_{kl}(s)\Psi(s)}{1+M(s)\left(K+s/R\right)G(s)}}_{\mathrm{OLTF}^{re}_{w\mathrm{IAC}}(s)}=0. \tag{36}$$

Based on the rearranged open-loop transfer function $\mathrm{OLTF}^{re}_{w\mathrm{IAC}}(s)$ in (36), the root locus plots relating to the available number of IACs S_{ON} can be obtained, as shown in Fig. 4. It can be seen from Fig. 4(a) that all the root loci are in the left-half plane. This indicates that the power system is stable regardless of the value of S_{ON}.

However, when the communication latency is considered, the power systems will be stable with some conditions, as shown in Fig. 4(b)–(d). Here the *Padé* approximant is set as $k=l=5$, i.e., the 5th-order approximant. Fig. 4(b)–(d) shows that the root loci will go from the left-half plane to the right-half plane with the increasing number of IACs providing regulation capacities. That is to say, if the communication latency is non-negligible in actual power systems, there exists a maximum number constraint of IACs ($S^{\max}_{\mathrm{ON},\tau}$) for providing regulation service. If the IACs' number exceeds $S^{\max}_{\mathrm{ON},\tau}$, the power system will become unstable in any load disturbance scenario.

Moreover, it can be illustrated in Fig. 4(b)–(d) that the value of $S^{\max}_{\mathrm{ON},\tau}$ becomes smaller as latency time increases. Therefore, in the case of the power system with a longer communication latency, the maximum number of IACs for providing regulation capacities should be fewer. In other words, given the power system with the same number of IACs participating in regulation services, a longer latency time can make the power system more unstable. The impacts of communication latency will be further analyzed in the numerical studies in Section V.

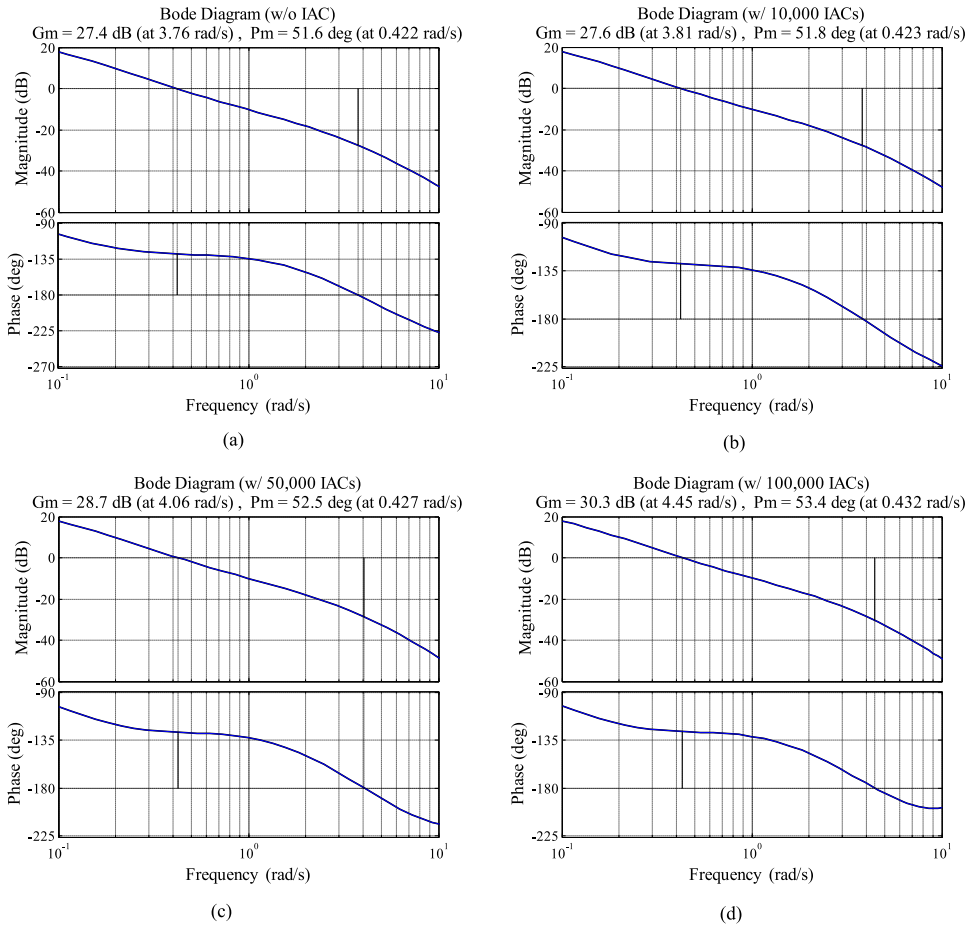

Fig. 3. Bode plots of the power system with and without IACs providing regulation capacities. (a) Without IAC. (b) With 10 000 IACs. (c) With 50 000 IACs. (d) With 100 000 IACs.

C. Sensitivity Analysis of the Power System With and Without IACs Providing Regulation Capacities

Sensitivity analysis is used to analyze the robustness of the power system faced with uncertain changes to the system parameters [25]. In this article, the sensitivity of the power system with regard to $M(s)$ is analyzed.

The derivative of the CLTF with respect to $M(s)$ can be calculated by (34). In order to simplify the theoretical derivation process, the functions $\mathrm{CLTF}_{w\mathrm{IAC}}(s)$ and $M(s)$ in (34) are substituted by y and x, respectively. The constant quantity is expressed as c. Therefore, (34) can be simplified as

$$y = \frac{-x}{1 + c \cdot x}. \tag{37}$$

The derivative of y with respect to x can be calculated as

$$\frac{\partial y}{\partial x} = \frac{-1 \cdot (1 + c \cdot x) - (-x) \cdot c}{(1 + c \cdot x)^2} = \frac{-1}{(1 + c \cdot x)^2}. \tag{38}$$

Then, the sensitivity of the proposed power system model with regard to $M(s)$ can be calculated as

$$\frac{\partial y}{\partial x} \Big/ \frac{y}{x} = \frac{-1}{(1 + c \cdot x)^2} \Big/ \frac{-1}{1 + c \cdot x} = \frac{1}{1 + c \cdot x} = \frac{x^{-1}}{x^{-1} + c}. \tag{39}$$

The (39) can also be expressed as

$$\begin{aligned} \mathbf{S}_{w\mathrm{IAC}}(s) &= \frac{\partial \mathrm{CLTF}_{w\mathrm{IAC}}(s)}{\partial M(s)} \Big/ \frac{\mathrm{CLTF}_{w\mathrm{IAC}}(s)}{M(s)} \\ &= \frac{M(s)^{-1}}{M(s)^{-1} + \left[\left(\frac{1}{R} + \frac{K}{s}\right) G(s) + \left(\delta + \frac{\gamma}{s}\right) P_{kl}(s) \Psi(s) S_{\mathrm{ON}}\right]}. \end{aligned} \tag{40}$$

Based on (35), the traditional power system model without IACs can also be calculated in the same method [from (37) to (39)], which is expressed as

$$\begin{aligned} \mathbf{S}_{wo\mathrm{IAC}}(s) &= \frac{\partial \mathrm{CLTF}_{wo\mathrm{IAC}}(s)}{\partial M(s)} \Big/ \frac{\mathrm{CLTF}_{wo\mathrm{IAC}}(s)}{M(s)} \\ &= \frac{M(s)^{-1}}{M(s)^{-1} + \left(\frac{1}{R} + \frac{K}{s}\right) G(s)}. \end{aligned} \tag{41}$$

Based on the (40) and (41), the sensitivity values of the power system with regard to $M(s)$ can be simulated, as shown in Fig. 5. It can be seen that the power system will be less sensitive to $M(s)$ with the increasing number of IACs for providing regulation services. From this perspective, the IACs can increase the robustness of the power system to deal with uncertain changes to the system parameters, e.g., D and H.

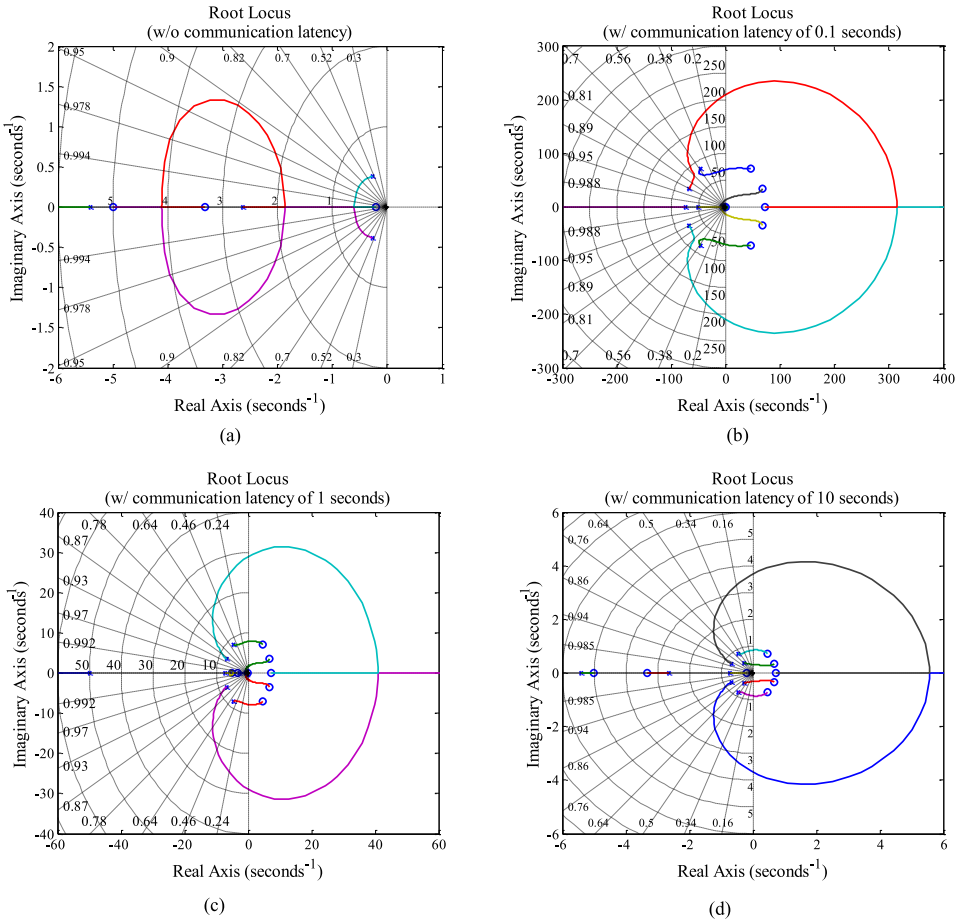

Fig. 4. Root locus plots of the power system with the increasing number of IACs providing regulation capacities. (a) Without communication latency. (b) With $\tau = 0.1$ s. (c) With $\tau = 1$ s. (d) With $\tau = 10$ s.

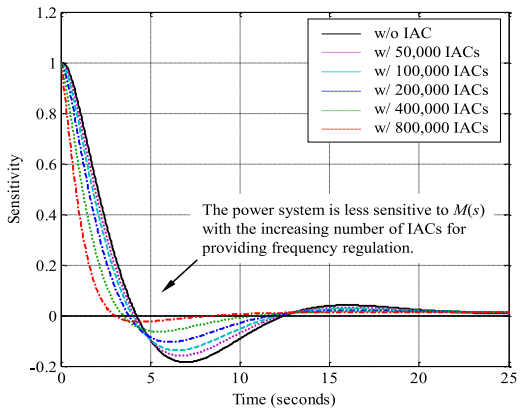

Fig. 5. Sensitivity values of the power system with regard to the system transfer function $M(s)$ under different numebr of IACs for providing regulation capacties without communication latency.

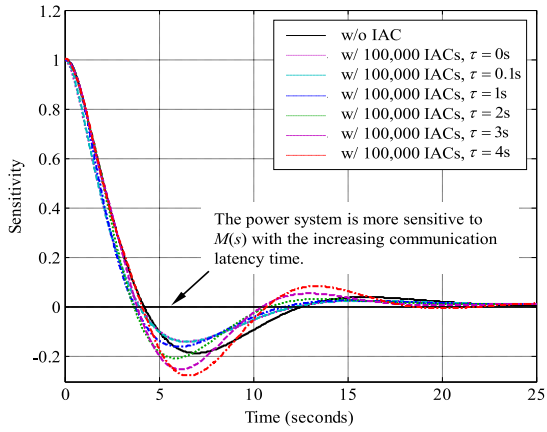

Fig. 6. Sensitivity values of the power system with regard to the system transfer function $M(s)$ under the same number of IACs for providing regulation capacities with different communication latencies.

However, when the communication latency between the occurrence time of the system frequency deviations and the action time of IACs cannot be neglected, the sensitivity values of the power system with the control loop of IACs ($\mathbf{S}_{w\mathrm{IAC}}$) may not be better than the original power system without IACs ($\mathbf{S}_{wo\mathrm{IAC}}$). As shown in Fig. 6, if there are 100 000 IACs in the control loop, the sensitivity values $\mathbf{S}_{w\mathrm{IAC}}$ will be less than $\mathbf{S}_{wo\mathrm{IAC}}$ only when the latency time is less than 1 s. The $\mathbf{S}_{w\mathrm{IAC}}$ will be larger than $\mathbf{S}_{wo\mathrm{IAC}}$ under $\tau = 2$, 3, and 4 s scenarios, which illustrate that the robustness of the power system decreases even though the IACs can increase the total regulation capacities.

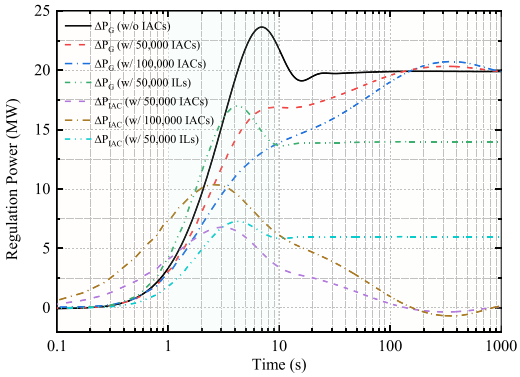

Fig. 7. Regulation power provided by the generator, the IACs, and the ILs.

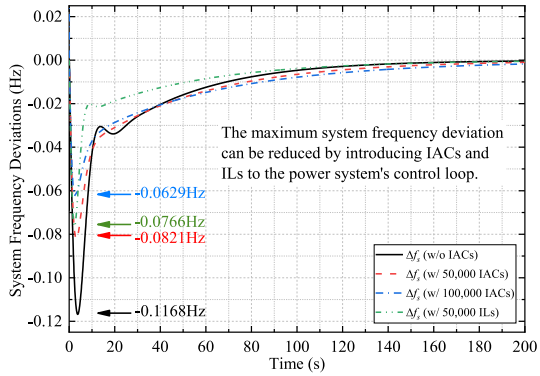

Fig. 8. System frequency deviations in the four cases.

In summary, IACs can indeed increase the robustness of power systems by providing regulation capacities, as shown in Fig. 5. However, this benefit is under the premise of small communication latency time, as shown in Fig. 6.

V. Case Studies

A. Test System

The power system in Fig. 2 is taken as the test system in this article, which includes a reheat steam generator, traditional loads, and IACs for providing regulation capacities. The parameter values are based on the data in Table I [15], [16]. The system capacity is 800 MW, and the rated frequency is 50 Hz. It is assumed that the initial load power is around 600 MW, and the disturbance power is 20 MW. Four cases are considered, namely: the regulation capacities are provided only by the generator in Case 1, by the generator and 50 000 IACs in Case 2, by the generator and 100 000 IACs in Case 3, and by the generator and 50 000 interruptible loads (ILs) in Case 4.

Therefore, the impacts of the IACs can be analyzed by comparing Case 1 and Case 2. The impacts of different number of IACs can be compared through Case 2 and Case 3. Besides, the 50 000 ILs in Case 4 are the same 50 000 IACs as those in Case 2, while the IACs in Case 4 are controlled by switching between ON- and OFF-states. The purpose here is to compare the control method proposed in this article (i.e., adjusting the compressor's operating frequency) with the traditional ON–OFF control method discussed in previous studies [3], [25], [26].

All the models and methods are formulated in MATLAB R2014a on a laptop with Intel(R) Core(TM) i7-5500U processors, clocking at 2.40 GHz and 8 GB RAM.

B. Dynamic Performances of the Regulation Process

Fig. 7 shows the regulation power provided by the generator, the IACs, and the ILs in the four aforementioned cases. Note that the horizontal axis employs log10 of the time to show both the details before 10 s and the adjustment results after 1000 s. It can be seen from the first 10 s in Fig. 7 that the IACs can be regulated more rapidly than the generator, which is helpful to decrease the power gap between generation and consumption to reduce system frequency deviations. Besides, it can be seen from the 100–1000 s in Fig. 7 that the generator finally undertakes all the regulation power, while the IACs smoothly withdraw from the regulation process. This confirms the analysis of the steady-state error evaluation in Section IV-A.

The system frequency regulation effects in the four cases can be found in Fig. 8, where the maximum frequency deviation can be reduced from −0.1168 Hz in Case 1 to −0.0821 Hz and −0.0629 Hz in Case 2 and Case 3, respectively. The variation of the maximum frequency deviation is significantly obvious between Case 1 and Case 2, which exactly benefits from the smaller regulation inertia of IACs relative to traditional generating units. This verifies the value of IACs for the stability of the power system—in agreement with the analysis in Section IV-B—even though the IACs withdraw all the regulation power with the recovery of the system balance.

Different from the control method discussed in this paper (i.e., continuously changing the compressor's operating frequency), the ILs in Case 4 are controlled by switching between ON- and OFF-states [3], [25], [26]. It can be seen from Fig. 7 that the ILs still maintain the regulation power (i.e., keeping the off-state) even though the system frequency deviations have been eliminated. Therefore, there is no doubt that the proposed control method in this article has less impact on end-user comfort, because it only changes the compressor's operating frequency within around 100 s.

In order to illustrate the impacts on end-user comfort in more detail, the indoor temperature deviations during the IACs' control process are shown in Fig. 9. It can be seen that the maximum indoor temperature deviation is around 0.16 °C, which has little impact on user comfort.

C. Impact Analysis of the Communication Latency and Padé Approximant

Latency time in the actual power system is based on various factors, for example, protocol, transmission distance, channel bandwidth, and network traffic [30]. Normally, power systems' state detection and data transmission are achieved via a wide-area measurement system (WAMS), in which the latency time includes measurement delay, data uplink delay, synchronization and calculation delay, data downlink delay, and controller action

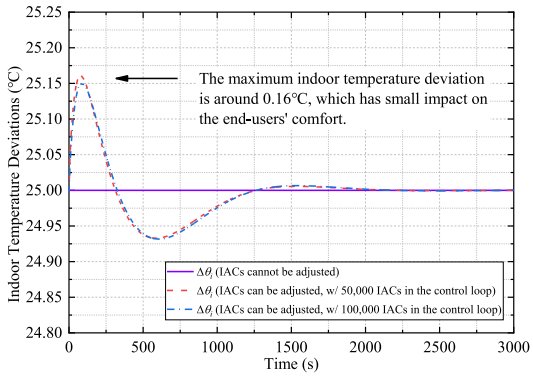

Fig. 9. Indoor temperature deviations when the IACs are in the control loop.

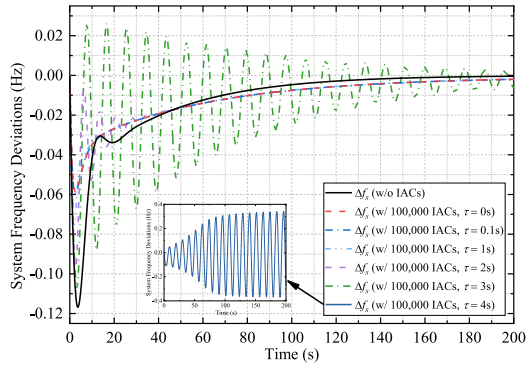

Fig. 10. System frequency deviations under different latency time.

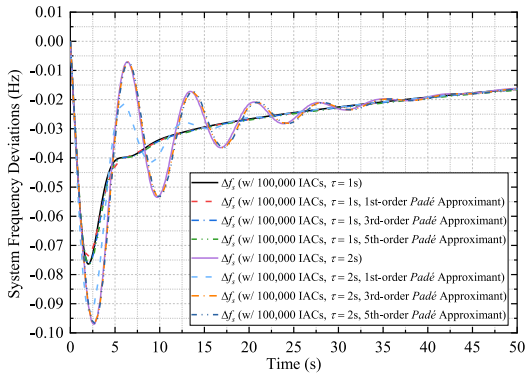

Fig. 11. Accuray of the *Padé* approximant for the communication latency.

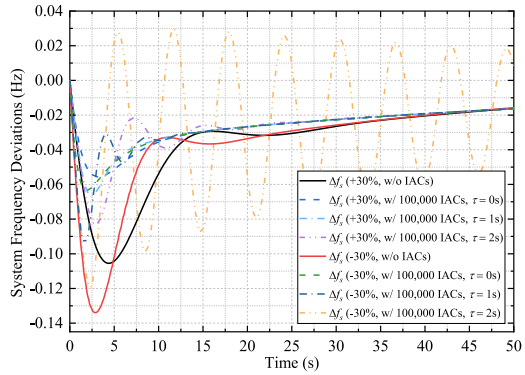

Fig. 12. Impact analysis of the system parameter uncertainties.

delay. In the US Pacific Northwest power system [31], the latency time of WAMS using fiber-optic digital communication is around 38 ms, and the latency time of WAMS using analog microwave channels is about 80 ms. In the Jiangsu Power Grid in China [32], the testing of WAMS latency time is in the range of 20–80 ms, and most of the latency time is within 40 ms. Besides, in the Guizhou Power Grid in China [33], the latency time of data transmission is measured around 10–20 ms, and the operational delays are in the ranges of 40–60 ms. Therefore, in actual power systems, the latency time is always less than 100 ms (i.e., less than 0.1 s).

Fig. 10 shows the system frequency deviations under different communication latencies ($\tau = 0$, 0.1, 1, 2, 3, and 4 s). It can be seen that the $\tau = 0.1$ s scenario nearly overlaps with the $\tau = 0$ s scenario, i.e., 0.1 s has almost no impact on regulation effects. This latency time is also the longest period of latency in actual power systems, for example, the US Pacific Northwest power system, the Jiangsu Power Grid and Guizhou Power Grid in China [31]–[33]. Under the $\tau = 1$ and 2 s scenarios, the maximum system frequency can still be reduced from -0.1168 to -0.0764 Hz and -0.0950 Hz, respectively. However, as the communication latency increases, the maximum system frequency deviation becomes closer to the scenario without IACs, and this comes with severe oscillations. More seriously, when the latency time reaches 4 s, the power system frequency cannot return to the stable state, as shown in the thumbnail in Fig. 10. Therefore, the communication latency had better be restricted to within 1 s to guarantee the benefit of IACs for the power system, which can be achieved easily by existing communication systems (generally, the latency time of actual WAMS is less than 0.1 s).

In order to verify the effectiveness of the *Padé* approximant, the 1st-, 3rd-, and 5th-order approximants are compared when the latency time is 1 and 2 s, as shown in Fig. 11. It can be seen that both the 3rd- and 5th-order approximants overlap with the ideal curves. Therefore, the 3rd-order *Padé* approximant is accurate enough to study the effects of the IACs' communication latency.

D. Impact Analysis of the System Parameter Uncertainties

In actual power systems, the system parameters (e.g., the load-damping factor D and the inertia constant H) cannot be measured and obtained so accurately. It is assumed that D and H have $\pm 30\%$ uncertainties around the nominal values. Total eight scenarios are compared in Fig. 12.

It can be seen that the power system with less D and H is more sensitive to disturbance power, mainly because of smaller system inertia. Besides, regardless of increases or decreases to these two system parameters, the IACs in the $\tau = 0$ s scenario always contribute to decreasing the system frequency deviations,

which confirms that the robustness of the power system gets enhanced by the IACs. However, with the extension of the communication latency, the regulation effectiveness of IACs becomes worse seriously, especially in the −30% scenarios. Therefore, in actual power systems with a high probability of communication latency, the minimum boundary values of the system parameters should be paid more attention, in order to set aside margins to guarantee system stability.

E. Experimental Test

Some realistic tests on the IAC (GREE KFR-72LW/(72555) FNhAd-A3) are carried out for providing regulation services for power systems. GREE is the largest air conditioning company and accounts for about forty percent of IAC sales in China (http://global.gree.com/). The GREE IAC is tested in a room of around 60 square meters, located in Hangzhou City, China. The adjustment ranges of the GREE compressor's frequency are around 10–90 Hz [15].

When the set temperature is 26 °C and the outdoor temperature is 5 °C, the GREE IAC is operating in the heating mode and the compressor's operating frequency is around 46 Hz. When the regulation service is needed and the controller send instructions to the IAC, the compressor's operating frequency decreases from around 46 to 30 Hz. Meanwhile, the IAC's operating power also drops from about 1800 to 750 W. The response time of the IAC is 11 s, which can meet the requirements of the response time for primary frequency regulation (i.e., 30 s).

VI. Conclusion

This article proposed a novel power system model with the control loop of large-scale IACs. The dynamic performances, stabilities, and sensitivities of the power system before and after considering IACs were analyzed and compared. The numerical results showed that the stability and robustness of the power system can be enhanced by the IACs, even though the IACs finally withdraw all the regulation power with the recovery of the system balance. However, the benefit of the IACs to the power system should satisfy the premise of limited communication latency. As for larger scale controlled IACs, the latency time should be restricted to a smaller value to avoid severe system oscillations. Finally, in power systems with uncertain parameters, the minimum boundary values should leave room for margins to guarantee system stability. The studies in this article can provide useful guidance for controlling IACs to provide regulation capacities for modern power systems.

In the future work, the authors will further focus on handling nonuniform time-varying delays and applying continuous consensus algorithms [34] in the proposed novel power system model with the control loop of IACs.

References

[1] N. Zhang, C. Kang, Q. Xia, and J. Liang, "Modeling conditional forecast error for wind power in generation scheduling," *IEEE Trans. Power Syst.*, vol. 29, no. 3, pp. 1316–1324, May 2014.

[2] J. Wang, H. Zhong, Q. Xia, and C. Kang, "Optimal planning strategy for distributed energy resources considering structural transmission cost allocation," *IEEE Trans. Smart Grid*, vol. 9, no. 5, pp. 5236–5248, Sep. 2018.

[3] H. Hui, Y. Ding, W. Liu, Y. Lin, and Y. Song, "Operating reserve evaluation of aggregated air conditioners," *Appl. Energy*, vol. 196, pp. 218–228, Jun. 2017.

[4] H. Zhong, Q. Xia, C. Kang, M. Ding, J. Yao, and S. Yang, "An efficient decomposition method for the integrated dispatch of generation and load," *IEEE Trans. Power Syst.*, vol. 30, no. 6, pp. 2923–2933, Nov. 2015.

[5] H. Hui, Y. Ding, Q. Shi, F. Li, Y. Song, and J. Yan, "5G network-based Internet of Things for demand response in smart grid: A survey on application potential," *Appl. Energy*, vol. 257, Jan. 2020, Art. no. 113972.

[6] M. Kuzlu, M. Pipattanasomporn, and S. Rahman, "Hardware demonstration of a home energy management system for demand response applications," *IEEE Trans. Smart Grid*, vol. 3, no. 4, pp. 1704–1711, Dec. 2012.

[7] P. Siano, "Demand response and smart grids—A survey," *Renew. Sust. Energy Rev.*, vol. 30, pp. 461–478, Feb. 2014.

[8] Y. Wang, Q. Chen, C. Kang, M. Zhang, K. Wang, and Y. Zhao, "Load profiling and its application to demand response: A review," *Tsinghua Sci. Tech.*, vol. 20, no. 2, pp. 117–129, Apr. 2015.

[9] Q. Shi, F. Li, Q. Hu, and Z. Wang, "Dynamic demand control for system frequency regulation: Concept review, algorithm comparison, and future vision," *Electr. Power Syst. Res.*, vol. 154, pp. 75–87, Jan. 2018.

[10] Q. Hu, F. Li, X. Fang, and L. Bai, "A framework of residential demand aggregation with financial incentives," *IEEE Trans. Smart Grid*, vol. 9, no. 1, pp. 497–505, Jan. 2018.

[11] P. Siano and D. Sarno, "Assessing the benefits of residential demand response in a real time distribution energy market," *Appl. Energy*, vol. 161, pp. 533–551, Jan. 2016.

[12] M. Pipattanasomporn, M. Kuzlu, S. Rahman, and Y. Teklu, "Load profiles of selected major household appliances and their demand response opportunities," *IEEE Trans. Smart Grid*, vol. 5, no. 2, pp. 742–750, Aug. 2013.

[13] Q. Shi, F. Li, G. Liu, D. Shi, Z. Yi, and Z. Wang, "Thermostatic load control for system frequency regulation considering daily demand profile and progressive recovery," *IEEE Trans. Smart Grid*, vol. 10, no. 6, pp. 6259–6270, Nov. 2019.

[14] K. J. Kim, L. K. Norford, and J. L. Kirtley, "Modeling and analysis of a variable speed heat pump for frequency regulation through direct load control," *IEEE Trans. Power Syst.*, vol. 30, no. 1, pp. 397–408, May 2014.

[15] H. Hui, Y. Ding, and M. Zheng, "Equivalent modeling of inverter air conditioners for providing frequency regulation service," *IEEE Trans. Ind. Electron.*, vol. 66, no. 2, pp. 1413–1423, Apr. 2018.

[16] W. Cui *et al.*, "Evaluation and sequential dispatch of operating reserve provided by air conditioners considering lead-lag rebound effect," *IEEE Trans. Power Syst.*, vol. 33, no. 6, pp. 6935–6950, Nov. 2018.

[17] S. Shao, W. Shi, X. Li, and H. Chen, "Performance representation of variable-speed compressor for inverter air conditioners based on experimental data," *Int. J. Refrigeration*, vol. 27, no. 8, pp. 805–815, Dec. 2004.

[18] Y. C. Park, Y. C. Kim, and M. K. Min, "Performance analysis on a multi-type inverter air conditioner," *Energy Conv. Manage.*, vol. 42, no. 13, pp. 1607–1621, Sep. 2001.

[19] Q. Zhang, Q. Guo, and Y. Yu, "Research on the load characteristics of inverter and constant speed air conditioner and the influence on distribution network," in *Proc. China Int. Conf. Electr. Distrib.*, 2016, pp. 1–4.

[20] N. Lu, "An evaluation of the HVAC load potential for providing load balancing service," *IEEE Trans. Smart Grid*, vol. 3, no. 3, pp. 1263–1270, Mar. 2012.

[21] P. Du and N. Lu, "Appliance commitment for household load scheduling," *IEEE Trans. Smart Grid*, vol. 2, no. 2, pp. 411–419, May 2011.

[22] M. Song, C. Gao, H. Yan, and J. Yang, "Thermal battery modeling of inverter air conditioning for demand response," *IEEE Trans. Smart Grid*, vol. 9, no. 6, pp. 5522–5534, Mar. 2017.

[23] J. Wang, C. Zhang, Y. Jing, and D. An, "Study of neural network PID control in variable-frequency air-conditioning system," in *Proc. Int. Conf. Control Autom.*, 2007, pp. 317–322.

[24] W. Viriyautsahakul, W. Panacharoenwong, W. Pongpiriyakijkul, S. Kosolsaksakul, and W. Nakawiro, "A simulation study of inverter air conditioner controlled to supply reactive power," *Proc. Comput. Sci.*, vol. 86, pp. 305–308, Jan. 2016.

[25] S. A. Pourmousavi and M. H. Nehrir, "Introducing dynamic demand response in the LFC model," *IEEE Trans. Power Syst.*, vol. 29, no. 4, pp. 1562–1572, Jul. 2014.

[26] V. P. Singh, P. Samuel, and N. Kishor, "Impact of demand response for frequency regulation in two-area thermal power system," *Int. Trans. Electr. Energy Syst.*, vol. 27, no. 2, pp. 1–23, Feb. 2017.

[27] J. Nanda, S. Mishra, and L. C. Saikia, "Maiden application of bacterial foraging-based optimization technique in multiarea automatic generation control," *IEEE Trans. Power Syst.*, vol. 24, no. 2, pp. 602–609, May 2009.
[28] Y. Bao, Y. Li, B. Wang, M. Hu, and P. Chen, "Demand response for frequency control of multi-area power system," *J. Modern Power Syst. Clean Energy*, vol. 5, no. 1, pp. 20–29, Jan. 2017.
[29] Y. Miao and D. Jiang, *Automatic Control Theory*, 2nd ed. Beijing, China: Tsinghua Univ. Press, 2013.
[30] B. Naduvathuparambi, M. C. Valenti, and A. Feliachi, "Communication delays in wide area measurement systems," in *Proc. 34th Southeastern Symp. Syst. Theory*, 2002, pp. 118–122.
[31] C. W. Taylor, V. Venkatasubramanian, and Y. Chen, "Wide-area stability and voltage control," in *Proc. 7th Symp. Specialists Electr. Oper. Expansion Planning*, 2002, pp. 1–9.
[32] Z. Hu, X. Xie, J. Xiao, and L. Tong, "Analysis and test on delays in the wide area measuring system," *Autom. Elect. Power Syst.*, vol. 28, no. 15, pp. 39–43, 2004.
[33] F. Zhang, Y. Sun, L. Cheng, X. Li, J. H. Chow, and W. Zhao, "Measurement and modeling of delays in wide-area closed-loop control systems," *IEEE Trans. Power Syst.*, vol. 30, no. 5, pp. 2426–33, Oct. 2014.
[34] R. Olfati-Saber, J. A. Fax, and R. M. Murray, "Consensus and cooperation in networked multi-agent systems," *Proc. IEEE*, vol. 95, no. 1, pp. 215–33, Mar. 2007.

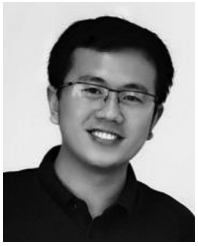

Hongxun Hui (Student Member, IEEE) received the bachelor's degree in electrical engineering, in 2015, from Zhejiang University, Hangzhou, China, where he is currently working toward the Ph.D. degree in electrical engineering.

He was elected in the first batch of the Academic Rising Star Program at Zhejiang University in 2018. His research interests include modeling and optimal control of demand-side resources in the smart grid, the electricity market considering demand response, and the uncertainty analysis brought by flexible loads and renewable energies.

Yi Ding (Member, IEEE) received the bachelor's degree from Shanghai Jiaotong University, Shanghai, China, in 2000, and the Ph.D. degree from Nanyang Technological University, Singapore, in 2007, both in electrical engineering.

He is a Professor of Reliability Analysis and Electricity Market with the College of Electrical Engineering, Zhejiang University, Hangzhou, China. His current research interests include power systems reliability/performance analysis incorporating renewable energy resources, smart grid performance analysis, and engineering systems reliability modeling and optimization.

Tao Chen (Member, IEEE) received the B.S. degree from Anhui University, Hefei, China, in 2012, the M.S. degree from the Tampere University of Technology, Tampere, Finland, in 2014, and the Ph.D. degree from the University of Michigan–Dearborn, Dearborn, MI, USA, in 2018, all in electrical engineering.

He was a Postdoc with Virginia Tech from 2018 to 2019. He is currently a Lecturer of Electricity Market and Machine Learning with the School of Electrical Engineering, Southeast University, Nanjing, China. His research interests include power systems, demand side management, and electricity market.

Saifur Rahman (Life Fellow, IEEE) received the B.Sc. degree from the Bangladesh University of Engineering and Technology, Dhaka, Bangladesh, in 1973, and the Ph.D. degree from Virginia Polytechnic Institute and State University, VA, USA, in 1978, both in electrical engineering.

He is the Director of the Advanced Research Institute, Virginia Polytechnic Institute and State University, Blacksburg, VA, USA, where he is the Joseph Loring Professor of Electrical and Computer Engineering and also directs the Center for Energy and the Global Environment. He served as the President of IEEE Power & Energy Society for 2018 and 2019. He was the Vice President of the IEEE Publications Board and as a member of the IEEE Board of Directors in 2006. He was the Founding Editor-in-Chief of the IEEE TRANSACTIONS ON SUSTAINABLE ENERGY and IEEE Electrification Magazine. He is a Distinguished Lecturer of the IEEE Power and Energy Society. From 1996 to 1999, he was a Program Director with the Engineering Directorate of the National Science Foundation. He has authored or coauthred in the areas of his research interests which include smart grid, conventional and renewable energy systems, load forecasting, uncertainty evaluation, infrastructure planning, and IoT device integration.

Dr. Rahman is a Member-at-Large of the IEEE-USA Energy Policy Committee.

Yonghua Song (Fellow, IEEE) received the B.Eng. and Ph.D. degrees from the Chengdu University of Science and Technology (now Sichuan University), Chengdu, China, and China Electric Power Research Institute, Beijing, China, in 1984 and 1989, respectively, both in electrical engineering, and the D.Sc. degree from Brunel University, Uxbridge, U.K., the Honorary Deng degree from the University of Bath, Bath, U.K., and the Honorary D.Sc. degree from the University of Edinburgh, Edinburgh, U.K.

He is currently the Rector of the University of Macau, Macau, China, and the Director of the State Key Laboratory of Internet of Things for Smart City, and also an Adjunct Professor with the Department of Electrical Engineering, Tsinghua University, Beijing, China, and the College of Electrical Engineering, Zhejiang University, Hangzhou, China.

Dr. Song is a Fellow of the Royal Academy of Engineering and a foreign member of Academia Europaea.